

Experimental Limits on the Nucleon Lifetime for Two- and Three-Body Decay Modes

H. S. Park, G. Blewitt, B. G. Cortez, G. W. Foster, W. Gajewski, T. J. Haines, D. Kielczewska, J. M. LoSecco, R. M. Bionta, C. B. Bratton, D. Casper, P. Chryscopoulou, R. Claus, S. Errede, K. S. Ganzezer, M. Goldhaber, T. W. Jones, W. R. Kropp, J. G. Learned, E. Lehmann, F. Reines, J. Schultz, S. Seidel, E. Shumard, D. Sinclair, H. W. Sobel, J. L. Stone, L. R. Sulak, R. Svoboda, J. C. van der Velde, and C. Wuest

The University of California at Irvine, Irvine, California 92717, and The University of Michigan, Ann Arbor, Michigan 48109, and Brookhaven National Laboratory, Upton, New York 11973, and California Institute of Technology, Pasadena, California 91125, and Cleveland State University, Cleveland, Ohio 44115, and The University of Hawaii, Honolulu, Hawaii 96822, and University College, London WC1E 6BT, United Kingdom, and Warsaw University, Warsaw PL-00-681, Poland

(Received 4 October 1984)

Lower limits in the range of 10^{31} to 10^{32} yr for the partial lifetimes of a number of nucleon decay modes are obtained from a 204-live-day exposure in an 8-ktonne water Cherenkov detector (3.3 ktonne in the fiducial volume). During this period 169 contained events were observed at a rate and with characteristics consistent with expected backgrounds from atmospheric ν interactions. Nine of the contained events are compatible with either a ν interaction or nucleon decay into a number of non- ν modes.

PACS numbers: 13.30.Ce, 11.30.Er, 14.20.Dh

The possibility of the nonconservation of baryon number arises in most attempts to unify the fundamental forces of nature.¹ The simplest of the grand unified theories (GUT's), minimal SU(5),² predicts the proton decay mode $p \rightarrow e^+ \pi^0$ at a rate³ inconsistent with experiment.⁴ It was recently suggested,⁵ however, that final-state interactions due to strong meson-field couplings may suppress the proton lifetime by about an order of magnitude. It remains to be seen whether further developments will narrow or increase the gap between theory and experiment.

The Irvine-Michigan-Brookhaven (IMB) detector has been described in previous Letters.⁴ The total volume of the detector is 8 ktonne and the fiducial volume is 3.3 ktonne (2.0×10^{33} nucleons). Charged particles above a critical velocity (0.75c) are detected by their Cherenkov light impinging on the photomultiplier tubes (PMT's). Electrons from muons which stop in the detector are identified with an efficiency $\sim 65\%$. The particles μ^\pm , π^\pm , and K^\pm are visible above total-energy thresholds of 160, 215, and 750 MeV, respectively. By contrast, e^\pm , γ , and π^0 's produce electromagnetic showers in which essentially all of their energy is deposited in the detector. The total light yield of an event (E_C , the Cherenkov equivalent energy) is obtained after correction for light attenuation in water, PMT angular response, pulse-height nonlinearity, and other systematic effects. The absolute scale of E_C is set by throughgoing muons which emit a known amount of Cherenkov light.

Charged pions produced in nucleon decays can interact in the water (interaction length ~ 28 cm at $E = 350$ MeV) introducing large fluctuations in light yield. For nucleon decays occurring inside oxygen nuclei the effects of Fermi motion and meson interac-

tions inside the nucleus must be considered. We use the intranuclear cascade model similar to the one described by Jones *et al.*⁶ to determine the types and energies of particles which ultimately escape the oxygen nucleus.

Data reduction procedures have been described previously.^{4,7} In the search for nucleon decay we first require that N_{PMT} , the number of illuminated PMT's, be in the range $40 \leq N_{\text{PMT}} \leq 300$. The mean N_{PMT} for decay modes with maximum light yields of ~ 1 GeV, e.g., $p \rightarrow e^+ \gamma$, is ~ 180 , so that the efficiency of the N_{PMT} requirement is $\geq 95\%$ for such modes. For decay modes with a low Cherenkov light yield, this efficiency can be low, e.g., $p \rightarrow \mu^+ \rho^0$ has an efficiency of $\sim 35\%$. We use the timing and the topology of the PMT's that fired to determine the event vertex. The mean error of the vertex determination varies between 0.5 and 1.0 m for various nucleon decay modes. The efficiency of the vertex-finding procedures is $> 80\%$, as determined by simulations of nucleon decays and ν interactions, as well as by laser-driven light sources which simulate single- and two-track events in the detector. Events passing the above requirements (2-3 events/live day) are scanned by physicists on a color graphics display.

A total of 169 events originated inside the fiducial volume during 204 days of live time. The vertices of 24 events were adjusted by hand with use of the color graphics system.

The search for a specific nucleon decay mode proceeds by making requirements on two characteristics of nucleon decay: (1) total energy, E_C (ideally 940 MeV, but modified for a given decay mode by the effects of Cherenkov thresholds, π absorption, and missing ν 's); and (2) total vector momentum ($p = 0$

for the decays originating in hydrogen, $p \leq 225$ MeV/c in oxygen) due to Fermi motion. In addition, we require the presence or absence of an observed muon decay as appropriate for the mode under consideration. Finally, for the four decay modes which should possess a clear two-body decay signature, viz. $p \rightarrow e^+ \gamma$, $p \rightarrow \mu^+ \gamma$, $p \rightarrow e^+ \pi^0$, $p \rightarrow \mu^+ \pi^0$, we require that two clearly defined tracks with opening angles $\geq 140^\circ$ be recognized on the graphics display, and include an efficiency factor evaluated by scanning of simulated events.

As a measure of the visible momentum balance we define a parameter A ("anisotropy") which is the magnitude of the vector sum of the unit vectors from the fitted vertex to each lit PMT, normalized by the total number of lit PMT's. For the events with a single short track A is ~ 0.7 (the cosine of the Cherenkov angle), and for isotropic or wide-angle two-body decay modes $A \leq 0.3$.

A scatter plot of E_C vs A for the 169 contained events from 204 live days is given in Fig. 1(a). As an example Fig. 1(b) is the same plot for one nucleon de-

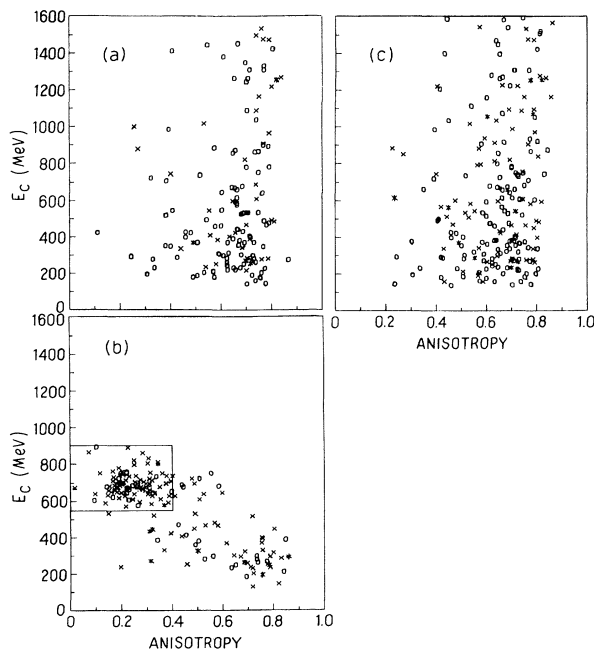


FIG. 1. (a) E_C vs A for the 169 contained events from 204 live days of data. Events with zero, one, and two identified $\mu \rightarrow e$ decays are indicated by circles, crosses, and asterisks, respectively. (b) E_C vs A for a representative simulated nucleon decay mode, $p \rightarrow \mu^+ \pi^0$. The spread is largely due to the π interactions in oxygen. The square box indicates the region from which candidates are accepted for this mode. (c) E_C vs A for a simulation of 204 days of atmospheric ν interactions. The number of background events for each mode given in Table I was determined from a 5-year ν simulation.

cay mode, $p \rightarrow \mu^+ \pi^0$. The enclosed region indicates the E_C and A requirements used to identify candidate events for this decay mode. Requirements for different decay modes are given in Table I.

We have investigated the effects on lifetime limits arising from possible systematic errors on E_C ($\pm 15\%$) and A (± 0.05). In all cases these errors produce changes in the 90% C.L. lifetime limits which are less than a factor of 2. The overall detection efficiencies (normalized to the fiducial mass) are presented in two forms: (a) with all nuclear effects included (column 6)—we use this efficiency to obtain our lifetime limits in column 10; and (b) with only Fermi motion and π^\pm interactions in the surrounding water taken into account (column 7 of Table I)—this is useful to relate our efficiencies to those of other experiments in a way which does not depend on the nuclear model.

Column 8 of Table I presents the number of contained events passing all the requirements for each nucleon-decay mode. Some events are "candidates" for more than one mode. The nine events passing all the requirements for non- ν modes are listed in Table II. For some modes with ν 's in the final state, there are a large number of candidates because of the momentum imbalance which is frequently mimicked by atmospheric ν interactions.

The background estimated from atmospheric ν interactions (column 9 of Table I) is simulated with use of the atmospheric ν flux calculations of Ref. 9. To obtain topologies and track energies for input to the detector simulation we use bubble-chamber ν data as described in Ref. 7. The simulated events were passed through the same analysis chain as the data to produce Fig. 1(c). The number of background events expected for each decay mode has been obtained by making identical requirements (E_C , A , μ decay, and where applicable, two-track topology) and is listed in column 9 of Table I.

Difficulties in estimation of backgrounds arise from the uncertainties in (a) the ν flux calculations ($\pm 30\%$); (b) charged- and neutral-current cross sections at $E_\nu \sim 1$ GeV; (c) possible scanning biases and the bubble-chamber detection efficiency for neutral particles (γ or n); (d) nuclear effects from π absorption which may differ significantly between water and the bubble-chamber liquids; (e) ambiguity in the identification of π^+ and p in the bubble-chamber data; (f) possible contamination of the bubble-chamber data by entering particles. Uncertainties (a) and (b) are partly addressed by the fact that the number of contained events agrees well (within 5%) with the predicted rate. To investigate (c) and (d), we have processed bubble-chamber data from three different experiments using three different liquids (CF_3Br , Ne, and D_2). Concerning the difficulty (e), we simulated background using different assumptions regarding the π^+/p identifica-

TABLE I. IMB nucleon-decay partial lifetime limits. Note the following points:

Column 1. For three-body decay modes flat phase space was assumed. For the cases marked with daggers, K_L^0 decays are included.

Columns 2-4. Different requirement regions correspond to different meson decay modes.

Column 4. Number of muon decay signals required.

Column 5. Number of events rejected by requiring two clear tracks with opening angle $> 140^\circ$. Efficiencies of columns 6 and 7 include a 90% scanning efficiency for this requirement.

Column 8. Some events are candidates for more than one mode. The letters a through i represent the candidate events listed in Table II.

Column 10. Lifetime limits quoted are at 90% C.L. for 204 live days and do not include background subtraction. See Ref. 8 for the procedure used to combine limits for modes with more than one requirement region.

1 Mode	3 Requirements				5 Back to Back	6 Effic. with Nuclear Corr.	7 Effic. without Nuclear Corr.	8 Candidates Observed	9 No. of Bkgnd. Est. -50%, +100%	10 Limit on τ/B ($\times 10^{31}$ yr) 90% C.L.
	2 E_C (MeV)	A	# μ	4						
p \rightarrow e $^+$ γ	750-1100	< 0.3	0	0	0.66	0.66	0	0.1	18.	
p \rightarrow e $^+$ π^0	750-1100	< 0.3	0	0	0.46	0.75	0	0.1	12.	
\dagger p \rightarrow e $^+$ K^0	300-500	< 0.5	1		0.12	0.12	i	2		
	750-1100	< 0.3	0		0.14	0.14	0	0.2	4.9	
p \rightarrow e $^+$ η^0	750-1100	< 0.3	0		0.37	0.54	0	0.2		
	400-650	< 0.5	1		0.07	0.15	0	2	12.	
p \rightarrow e $^+$ ρ^0	200-600	0.1-0.5	1		0.16	0.30	i	4	2.5	
p \rightarrow e $^+$ ω^0	300-600	0.1-0.5	1		0.19	0.39	i	3		
	750-1100	< 0.3	0		0.05	0.06	0	0.2	4.0	
p \rightarrow μ^+ γ	550-900	< 0.5	1	2	0.52	0.52	0	0.4	14.	
p \rightarrow μ^+ π^0	550-900	< 0.4	1	1	0.32	0.44	b	0.2	5.1	
\dagger p \rightarrow μ^+ K^0	150-400	0.1-0.5	1,2		0.19	0.20	f, i	2		
	550-900	< 0.5	1		0.14	0.14	a, b	2	2.9	
p \rightarrow μ^+ η^0	550-900	< 0.5	1		0.23	0.44	a, b	2		
	200-400	< 0.5	1,2		0.12	0.22	f, i	2	3.1	
p \rightarrow μ^+ ρ^0	150-400	0.1-0.5	1,2		0.10	0.16	f, i	2	1.2	
p \rightarrow μ^+ ω^0	200-450	0.1-0.5	1,2		0.18	0.32	f, i	2		
	650-900	< 0.5	1		0.03	0.05	a, b	0.8	2.1	
p \rightarrow ν K^+	150-375	0.3-0.6	1		0.08	0.08	3	4	0.7	
p \rightarrow ν ρ^+	300-600	0.2-0.5	1		0.07	0.19	1	3	1.1	
p \rightarrow ν K^{*+}	250-500	0.3-0.6	1		0.09	0.19	4	4	0.7	
p \rightarrow e $^+$ e $^+$ e $^-$	750-1100	< 0.3	0		0.93	0.93	0	0.2	25.	
p \rightarrow μ^+ u $^+$ u $^-$	200-425	< 0.5	2,3		0.58	0.58	f	0.2	9.	
n \rightarrow e $^+$ π^-	450-950	< 0.5	0		0.40	0.55	c, e, g, h	4	2.5	
n \rightarrow e $^-$ π^+	400-700	< 0.5	1		0.10	0.24	0	2		
	700-950	< 0.5	0		0.10	0.07	c, e	2	2.5	
n \rightarrow e $^+$ ρ^-	400-800	< 0.4	0		0.20	0.42	c, d, e, g	2	1.2	
n \rightarrow e $^+$ π^+	400-800	< 0.4	0,1		0.22	0.57	a, c, d, e, g	3	1.2	
n \rightarrow μ^+ π^-	200-700	< 0.5	1		0.30	0.43	i	4	3.8	
n \rightarrow μ^+ π^+	200-500	< 0.5	1,2		0.29	0.45	f, i	3	2.7	
n \rightarrow μ^+ ρ^-	300-550	< 0.5	1		0.07	0.29	i	2	0.9	
n \rightarrow μ^+ ρ^+	300-550	< 0.5	1,2		0.10	0.41	f, i	2	0.9	
n \rightarrow ν γ	350-600	0.5 <	0		0.77	0.77	28	19	1.1	
n \rightarrow ν π^0	350-600	0.5 <	0		0.51	0.82	28	19	0.7	
n \rightarrow ν K^0	450-700	0.2-0.5	0		0.10	0.11	2	2	1.0	
n \rightarrow ν η^0	450-800	0.1-0.5	0		0.29	0.56	4	3	1.8	
n \rightarrow ν ρ^0	150-500	0.1-0.4	0,1		0.05	0.11	7	3	0.2	
n \rightarrow ν ω^0	200-450	0.2-0.5	1		0.08	0.24	1	2		
	650-950	< 0.3	0		0.03	0.06	0	0.3	1.6	
n \rightarrow ν K^{*0}	200-700	0.15-0.5	1		0.06	0.11	1	4	0.7	
n \rightarrow e $^+$ e $^-$ ν	500-850	< 0.5	0		0.41	0.41	4	3	2.6	
n \rightarrow μ^+ μ^- ν	150-375	0.2-.65	1,2		0.31	0.31	4	7	1.9	

tion ambiguity. On the basis of these considerations we assign an overall uncertainty of (-50%, +100%) to the background estimation for any given mode. No background subtraction was made in deriving the lifetime limits in Table I. Higher limits would be obtained with a background subtraction.

In conclusion, a survey of Table I shows that $\sim \frac{1}{2}$

of the modes are currently background limited at a lifetime limit of (a few) $\times 10^{31}$ yr. We expect that more detailed analysis of the energy and topology of events will reduce the expected background and therefore increase the sensitivity for many modes. For modes without candidates the present lifetime limits are $\sim 10^{32}$ yr.

TABLE II. Events passing all the requirements for non- ν modes.

Event No.	E_C (MeV)	Anisotropy A	No. of μ decays
a	143-21939	0.40	1
b	225-7794	0.27	1
c	299-72044	0.33	0
d	420-34248	0.11	0
e	510-54208	0.36	0
f	588-8320	0.50	2
g	656-11673	0.37	0
h	663-1770	0.41	0
i	747-44203	0.45	1

We wish to thank the many people who helped to bring the IMB detector into successful operation. We are grateful to our host, Morton-Thiokol Inc., who

operate the Fairport mine.

¹For a review of grand unified theories, see P. Langacker, *Phys. Rep.* **72**, 185 (1981).

²H. Georgi and S. L. Glashow, *Phys. Rev. Lett.* **32**, 438 (1974).

³W. J. Marciano, Brookhaven National Laboratory Report No. BNL 31036 (unpublished), presented at *Orbis Scientiae* 1982.

⁴R. M. Bionta *et al.*, *Phys. Rev. Lett.* **51**, 27 (1983).

⁵A. S. Goldhaber, T. Goldman, and S. Nussinov, *Phys. Lett.* **142B**, 47 (1984).

⁶T. W. Jones *et al.*, *Phys. Rev. Lett.* **52**, 720 (1984).

⁷B. Cortez *et al.*, *Phys. Rev. Lett.* **52**, 1092 (1984).

⁸B. Cortez, Ph.D thesis, Harvard University, 1983 (unpublished).

⁹T. K. Gaisser and T. Stanev, in *Proceedings of the International Colloquium on Baryon Nonconservation, Salt Lake City, January, 1984*, edited by D. Cline (Univ. of Wisconsin Press, Madison, 1984), p. 61; T. K. Gaisser, in *Proceedings of the Eleventh International Conference on Neutrino and Astro Physics*, edited by K. Kleinknecht and E. A. Paschos (World Scientific, Singapore, 1984), p. 372.